Nanoscale mechanical control of surface electrical properties of manganite films with magnetic nanoparticles – Electronic Supplementary Information (ESI)

Borislav Vasić,*[a] Zorica Konstantinović,[b] Elisa Pannunzio-Miner,‡[c] Sergio Valencia,[d] Radu Abrudan,¶[e] Radoš Gajić,[a] and Alberto Pomar[c]

[a] *Graphene Laboratory of Center for Solid State Physics and New Materials, Institute of Physics Belgrade, University of Belgrade, Pregrevica 118, 11080 Belgrade, Serbia; E-mail: bvasic@ipb.ac.rs*
[b] *Center for Solid State Physics and New Materials, Institute of Physics Belgrade, University of Belgrade, Pregrevica 118, 11080 Belgrade, Serbia*
[c] *Institut de Ciència de Materials de Barcelona, ICMAB-CSIC, Campus de la UAB, 08193 Bellaterra, Spain*
[d] *Helmholtz-Zentrum Berlin für Materialien und Energie, Albert-Einstein-Str.15, 12489 Berlin, Germany*
[e] *Institut für Experimentalphysik/Festkörperphysik, Ruhr-Universität Bochum, 44780 Bochum, Germany*

‡ *Present address: Centro de Investigaciones en Ciencias de la Tierra (CICTERRA-CONICET-UNC), Facultad de Ciencias Exactas, Físicas y Naturales, Av. Velez Sarfield 1611, X5016GCA Ciudad Universitaria, Cordoba, Argentina*
¶ *Present address: Helmholtz-Zentrum Berlin für Materialien und Energie, Albert-Einstein-Str.15, 12489 Berlin, Germany*

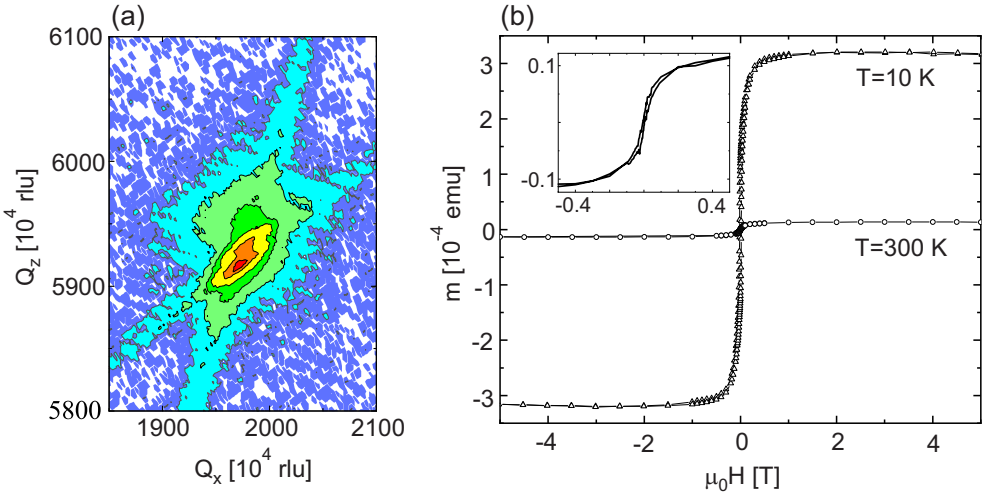

Figure S1: (a) Reciprocal space maps of (103) reflections of the LSMO film. (b) In-plane magnetization curves of the LSMO thin film with self-assembled FeO_x nanoparticles measured at 10 K and 300 K. The inset in (b): detail of the room temperature hysteresis loop. Low temperature magnetization curve (T = 10 K) is dominated by the signal from 100 nm thick LSMO film. On the other hand, the high temperature magnetization is very weak and the hysteresis is almost closed (H_c = 50 Oe). Taking into account the depressed value of the ferromagnetic transition (T_c = 270 K) in nanostructured manganite thin films [1], the magnetization curve at room temperature (T = 300 K) should arise from iron-based nanoparticles (notice that, at T = 300 K, the magnetization disappears in bare LSMO films and remains principally only in the film with FeO_x NPs as shown in Fig. S4(b)).

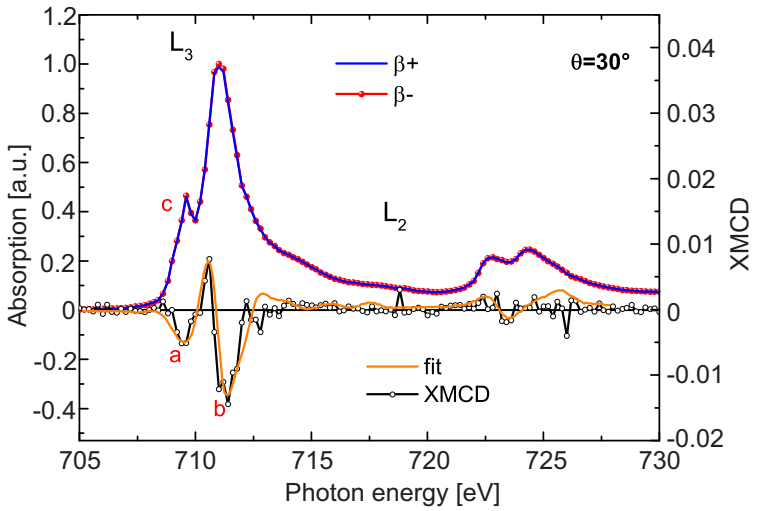

Figure S2: The results of XAS measurements ($\beta+$ and $\beta-$ curves) as well as the resulting XMCD. The XAS spectrum can be considered to be alike to the individual $\beta+$ and $\beta-$ curves due to the small dichroic effect (max ca. 1.5%). The Fe $L_{3,2}$-edge absorption curve is representative of a Fe^{3+} oxidation state [2]. More information can be obtained from the XMCD shape. More concretely, the strength of spectroscopic features a, b and c appearing at the L_3 edge of the XMCD of magnetic iron oxide compounds are known to depend on the Fe oxidation state and coordination of the Fe magnetic species, i.e. Fe^{2+} in octahedral coordination and Fe^{3+} in octahedral and tetrahedral coordination [3]. We have fit the experimental XMCD curve with reported XMCD curves for the individual contributions [3]. The best fit is in agreement with the XAS data pointing to a major Fe^{3+} contribution (92%), although a minute amount of Fe^{2+} needs to be considered in order to reproduce the intensity of the feature. The fit shows that 65% of Fe is in octahedral coordination (52.5% Fe^{3+} and 8.0% Fe^{2+}) while 39.5% in tetrahedral one. The XAS, the size of the effect as well as the fit results of the XMCD curve seem to indicate that we have a γ-Fe_2O_3 phase [4, 5, 6, 7].

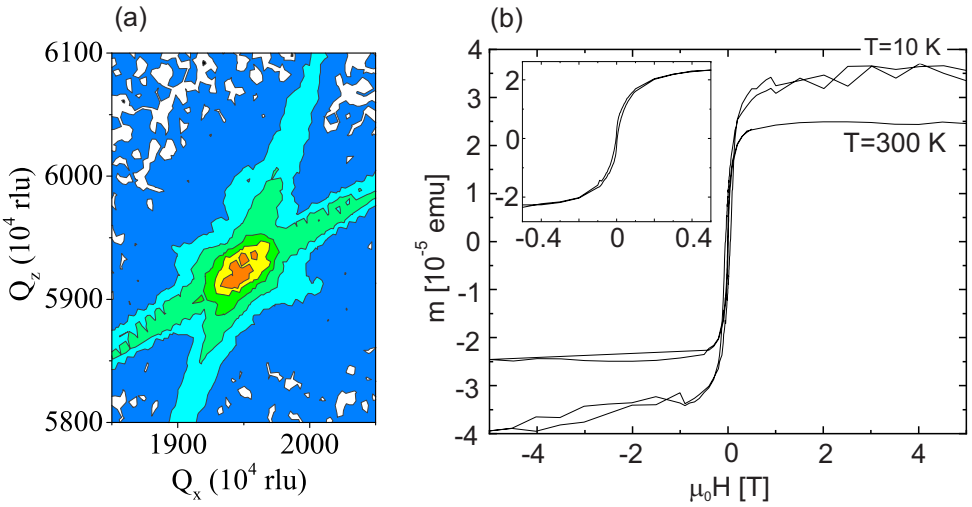

Figure S3: (a) The asymmetric reciprocal space map of (103) reflections of the 20 nm thick LSFMO film grown on top of the STO substrate. Although, the reflection from LSFMO (103) is low, the LSFMO film seems to be fully strained with in-plane lattice constant close to $a_{\parallel,\mathrm{STO}} = 3.905$ Å. Due to presence of tensile strain in the thin film, the out-of-plane parameter is reduced than the corresponding bulk value $a_{\mathrm{LSFMO}} = 3.873$ Å [8] and estimated to $a_{\perp,\mathrm{LSFMO}} = 3.862(8)$ Å. (b) In-plane magnetization curves of the 20 nm thick LSFMO film with self-assembled FeO_x NPs measured at 10 K and 300 K. The inset in (b): detail of the room temperature hysteresis loop typically found in disordered manganite thin films. On the other hand, the high temperature magnetization is very weak and the hysteresis is almost closed ($H_c = 50$ Oe). Taking into account that the ferromagnetic transition of LSFMO lies below the room temperature ($T_c = 270$ K), the magnetization curve at room temperature should arise, as in the previous case, from iron-based NPs (notice that, at T = 300 K, the magnetization disappears in bare LSFMO films and remains principally only in the film with FeO_x NPs as shown in Fig. S4(c)).

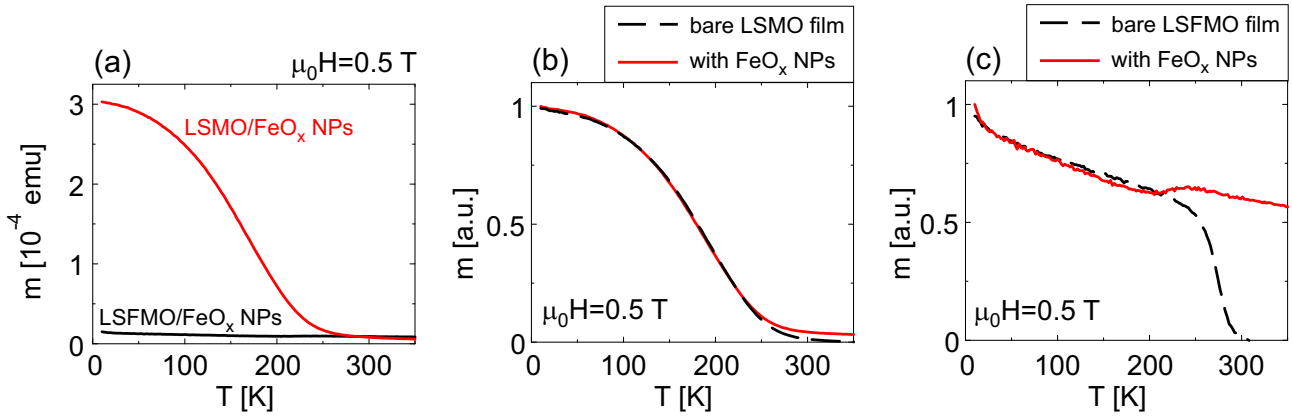

Figure S4: (a) In-plane magnetization curves of LSMO and LSFMO film with FeO_x NPs measured under H = 0.5 T. Comparison of the normalized magnetization of bare manganite films (dashed line) and the one with FeO_x NPs (solid line) for (b) LSMO (100 nm thick film) and (c) LSFMO (20 nm thick film). At 300 K, the magnetization disappears in bare manganite films and remains principally only in the structures with FeO_x NPs.

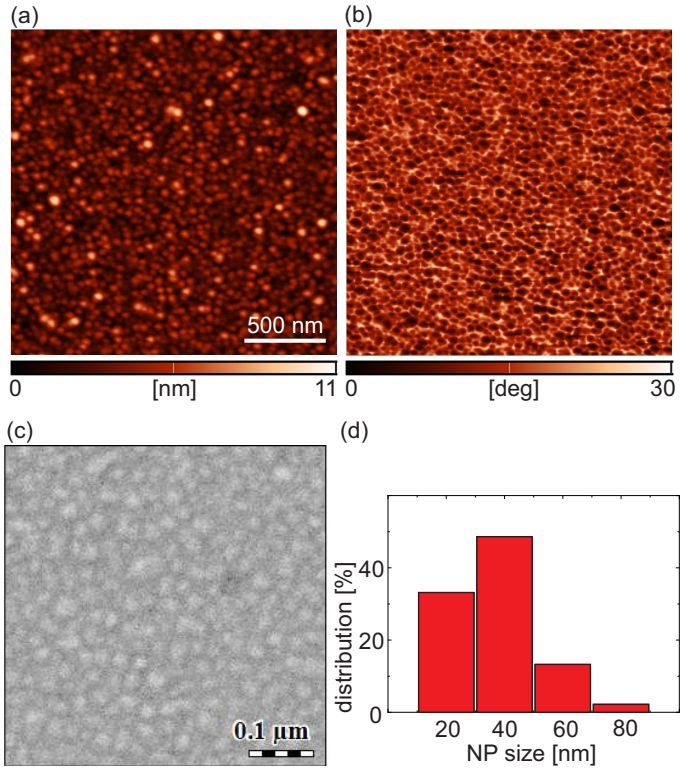

Figure S5: Morphology of the sample consisting of LSFMO film with iron-oxide NPs: (a) AFM topographic image and (b) the corresponding phase image of the sample acquired during the imaging in tapping mode, (c) SEM image and (d) the size distribution of iron-oxide NPs.

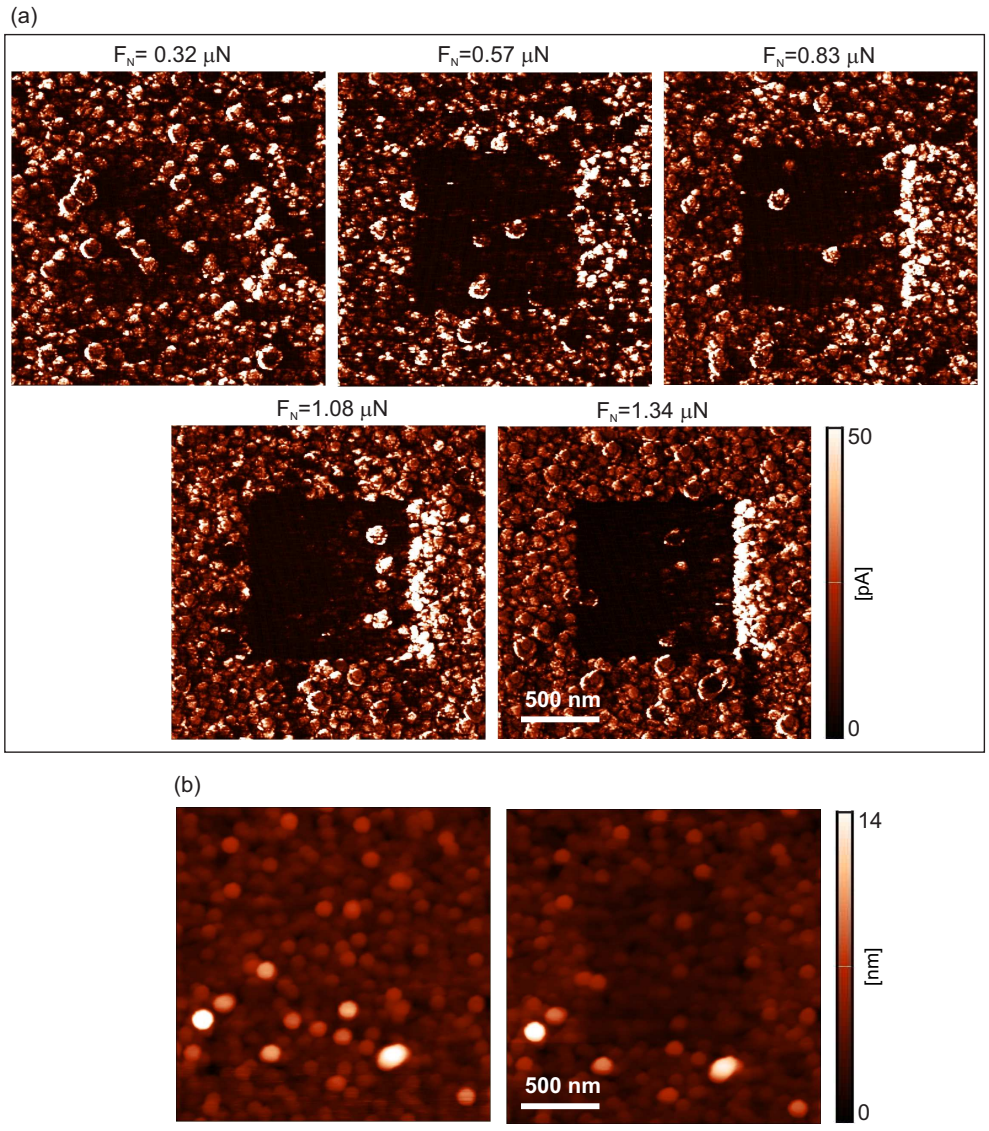

Figure S6: Conductivity of the sample consisting of LSFMO film with iron-oxide NPs: (a) 2×2 μm^2 current maps measured by C-AFM after the rubbing of inner 1×1 μm^2 domain at specified normal force, (b) Sample morphology before (the left image) and after (the right image) the rubbing of the inner square 1×1 μm^2 domain at the highest normal load of 1.34 μN.

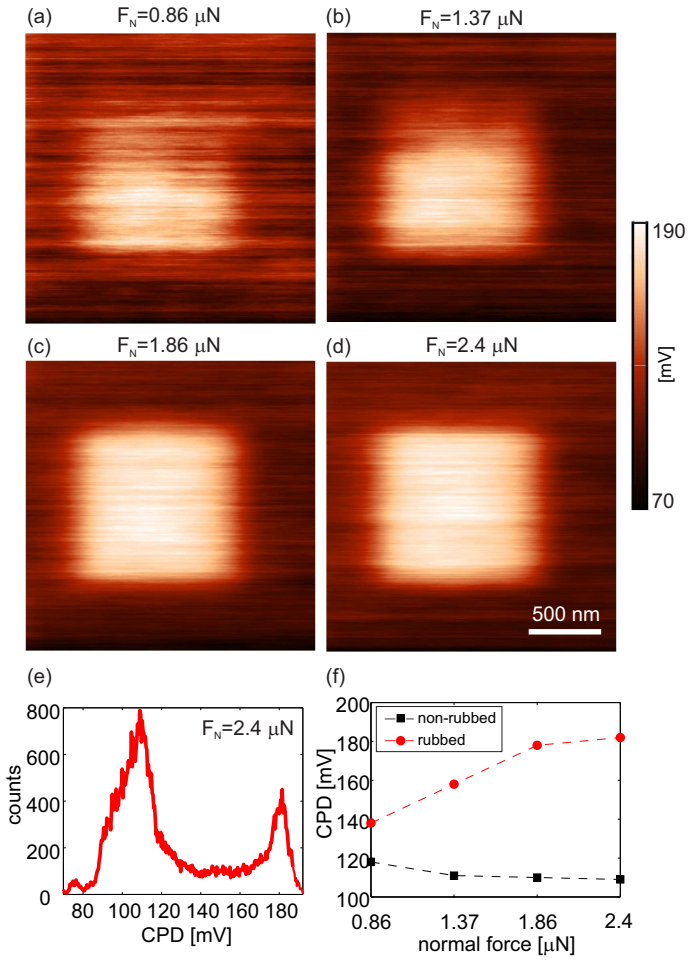

Figure S7: Electrical surface potential of the sample consisting of LSFMO film with iron-oxide NPs: (a-d) 2×2 μm^2 CPD maps measured by KPFM after the rubbing of inner 1×1 μm^2 domain at specified normal force, and (f) CPD change on rubbed and non-rubbed regions as a function of normal force.

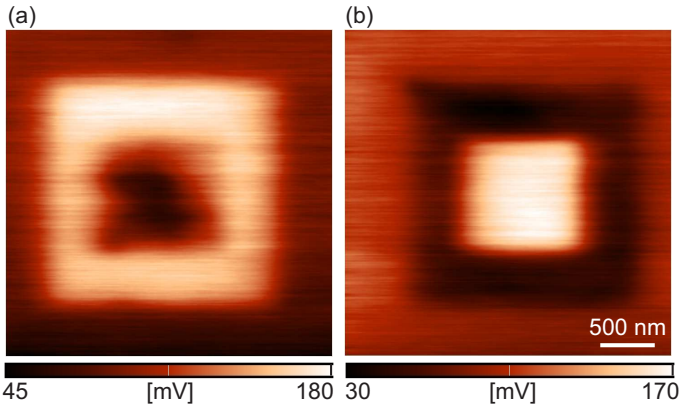

Figure S8: 3×3 μm^2 CPD maps of the sample consisting of LSFMO film with iron-oxide NPs, rubbed with both grounded (at high normal load) and biased (low normal load and negative bias voltage) tip: (a) first, the inner 2×2 μm^2 domain was rubbed by grounded AFM probe and at the normal force 0.48 μN, and then, the smaller inner 1×1 μm^2 domain was scanned in the contact mode at low normal force 0.16 μN and with tip bias voltage -1 V, and (b) first, the inner 2×2 μm^2 domain was scanned in the contact mode at low normal force 0.16 μN and with tip bias voltage -1 V, and then the smaller inner 1×1 μm^2 domain was rubbed by grounded AFM probe and at the normal force 0.48 μN.

References

[1] Z. Konstantinović, J. Santiso, Ll. Balcells, and B. Martínez. Strain-Driven Self-Assembled Network of Antidots in Complex Oxide Thin Films. *Small*, 5:265–271, 2009.

[2] T. J. Regan, H. Ohldag, C. Stamm, F. Nolting, J. Lüning, J. Stöhr, and R. L. White. Chemical effects at metal/oxide interfaces studied by x-ray-absorption spectroscopy. *Phys. Rev. B*, 64:214422, 2001.

[3] R. A. D. Pattrick, G. Van Der Laan, C. M. B. Henderson, P. Kuiper, E. Dudzik, and D. J. Vaughan. Cation site occupancy in spinel ferrites studied by X-ray magnetic circular dichroism: developing a method for mineralogists. *Eur. J. Mineral.*, 14:1095–1102, 2002.

[4] S. Brice-Profeta, M.-A. Arrio, E. Tronc, N. Menguy, I. Letard, C. Cartier dit Moulin, M. Noguès, C. Chanéac, J.-P. Jolivet, and Ph. Sainctavit. Magnetic order in $\gamma - Fe_2O_3$ nanoparticles: a XMCD study. *J. Magn. Magn. Mater.*, 288:354 – 365, 2005.

[5] E. Pellegrain, M. Hagelstein, S. Doyle, H. O. Moser, J. Fuchs, D. Vollath, S. Schuppler, M. A. James, S. S. Saxena, L. Niesen, O. Rogojanu, G. A. Sawatzky, C. Ferrero, M. Borowski, O. Tjernberg, and N. B. Brookes. Characterization of Nanocrystalline $\gamma - Fe_2O_3$ with Synchrotron Radiation Techniques. *Phys. Status Solidi B*, 215(1):797–801, 1999.

[6] D. H. Kim, H. J. Lee, G. Kim, Y. S. Koo, J. H. Jung, H. J. Shin, J.-Y. Kim, and J.-S. Kang. Interface electronic structures of $BaTiO_3$@X nanoparticles (X=$\gamma - Fe_2O_3$, Fe_3O_4, $\alpha - Fe_2O_3$, and Fe) investigated by XAS and XMCD. *Phys. Rev. B*, 79:033402, 2009.

[7] L. Cao, Z.-X. Jiang, Y.-H. Du, X.-M. Yin, S.-B. Xi, W. Wen, A. P. Roberts, A. T. S. Wee, Y.-M. Xiong, Q.-S. Liu, and X.-Y. Gao. Origin of Magnetism in Hydrothermally Aged 2-Line Ferrihydrite Suspensions. *Environ. Sci. Technol.*, 51:2643–2651, 2017.

[8] G. Zhang and J. Lin. Synthesis, electronic and magnetic properties of the double B mixed perovskite series $La_{0.5}Sr_{0.5}Mn_{1-x}Fe_xO_3$. *J. Alloys Compd.*, 507:47 – 52, 2010.